1. Background

Actin exists in a dynamic equilibrium between monomeric globular actin (G-actin) and polymerized filamentous actin (F-actin). The actin monomer comprises four subdomains arranged into inner and outer domains. Subdomains 1 and 3 define a hydrophobic cleft that plays a central role in actin polymerization by interacting with the D-loop of incoming monomers at the barbed (plus) end.

A diverse class of natural actin-targeting toxins exploits this structural feature to modulate actin dynamics. Filament-destabilizing toxins, including mycalolides, kabiramides, jaspisamides, aplyronines, and reidispongiolides, typically bind at the barbed-end interface. Many of these compounds share a common architectural motif: a large macrolactone ring that anchors the molecule to a shallow hydrophobic groove on actin, coupled to a projecting, largely hydrophobic tail that penetrates deeply into the barbed-end cleft.

2. Project goal

- Develop an end-to-end docking pipeline from ligand preparation through pose evaluation across multiple actin conformational states.
- Quantify steric clashes and physicochemical features of docked ligands and evaluate their relationship to experimental potency using a logistic regression model.
- Benchmark docking outcomes against crystallographic G-actin–ligand complexes using RMSD and contact-based metrics.

3. Pipeline overview

3.1 Ligand preparation

17 ligands were selected, including actin barbed-end binding natural toxins (11), tail analogues of the natural toxins (3), and negative controls of actin toxins binding to different sites (3). Use RDKit to generate 30 conformers per ligand, using a maximum of 300 iterations. Select 3 conformers per ligand to proceed to docking. Open Babel was used to transform the conformers into vina ready pdbqt form.

3.2 Receptor preparation

Structures were downloaded from PDB, and single chain was selected with PyMol. Preparation was done in AutoDock Tool to remove water molecules, add polar hydrogens, assign AD4 parameters, and Gasteiger charges was added to generate the pdbqt file for Vina docking.

3.3 Docking

Docking center and boxes were determined using published Mycalolide B-actin interaction. Large box was padded with 18 Å, and tight box used either 32 X 32 X 32 box, or 28 X 32 X 32 box. Docking itself was run with Autodock Vina, with 3 conformers per ligand, 10 poses each.

Docking using both AMPPNP binding actin protomer (6DJM, chain A) and ADP binding protomer (6DJO, chain A). The paper mentioned ADP-Pi binding form is not significantly different from the AMPPNP form, therefore, omitted from the test.

Docking affinity of the best pose per conformer per ligand was recorded ans used for significant test.

3.4 ChimeraX computation

Clashes between ligand and F-actin structure (labeled as chain A-C) was calculated with ChimeraX, using cutoff at 0.4, 0.6, and 0.8 Å. Clashes between ligand and receptor was also calculated to confirm the docking is not causing clashing.

RMSD was first calculated between X-ray results (6W7V) of **2a** as ground truth and docking results. Numbers are read by ChimeraX.

Contacts were calculated between X-ray results (2ASM) of Reidispongiolide A as ground truth and docking results. Only tail region of Reidispongiolide A (29 heavy atoms) was used for the computation.

3.5 Potency predictions

Clash results and ligand features generated with RDKit were used as input to train a logestic regression model, and ROC-AUC was used for accuracy readout.

4. Key result

4.1 Docking distinguishes barbed-end binders from negative controls

Docking results revealed a clear qualitative difference between known barbed-end binding toxins and negative control actin toxins that bind alternative sites. Negative controls such as latrunculin B (G-actin sequestration) and phalloidin (F-actin stabilization) produced dispersed docking poses across the protein surface, with no clear convergence. In contrast, bona fide barbed-end binding toxins (e.g., Mycalolide B) and tail-only analogs (e.g., **2a**) consistently docked into a localized region corresponding to the barbed-end cleft, forming a distinct pose cluster. This suggests that docking captures a meaningful energy basin for barbed end targeting ligands despite limitations in pose accuracy.

Latrunculin B (sequesters G-actin, Negative Control) dispersed docking position		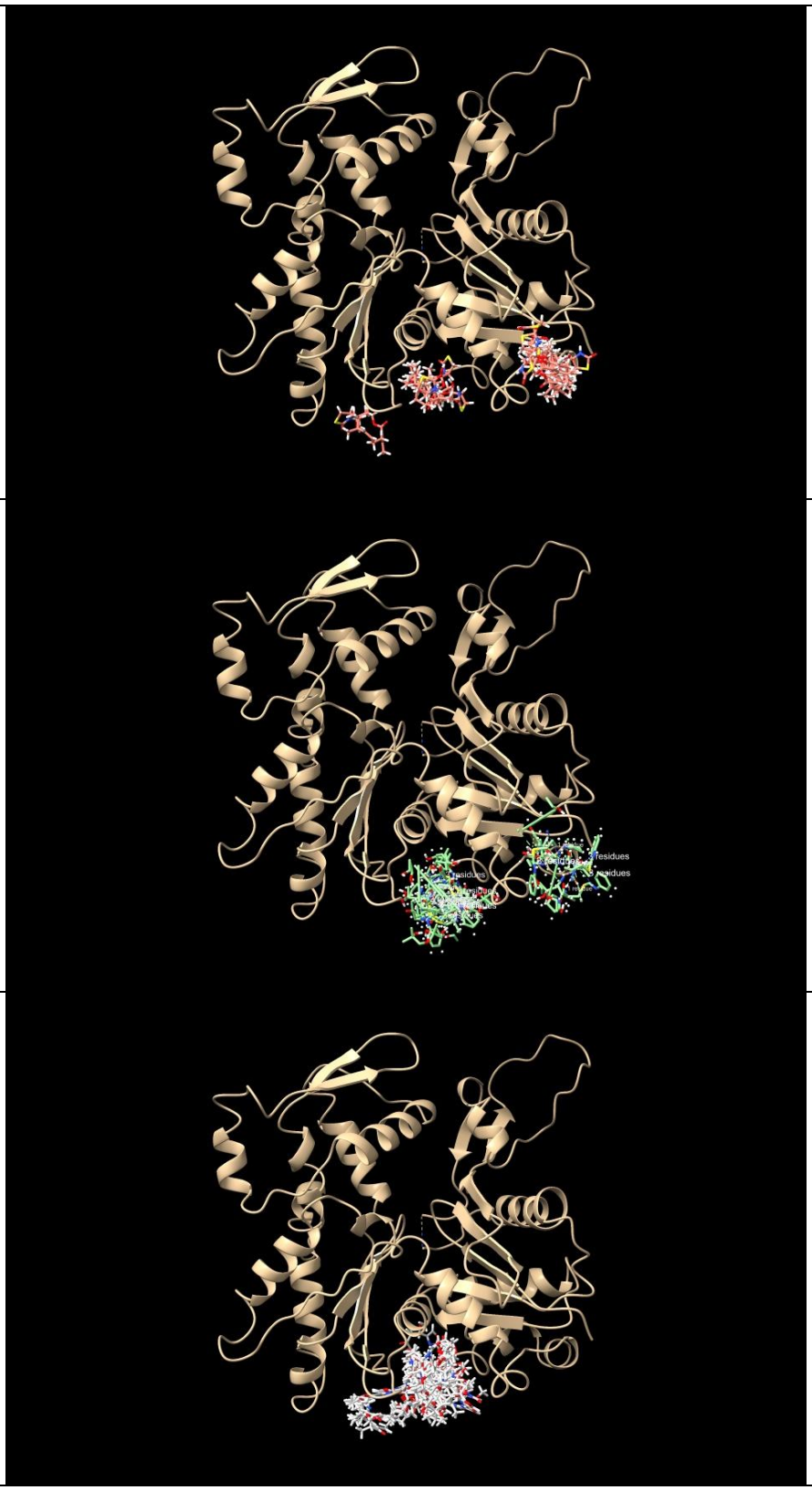
Phalloidin (stabilizes F-actin, Negative Control) dispersed docking position		
Mycalolide B (barbed-end binding toxin) Converged docking position		

2a (barbed-end binding analogue) Converged docking position		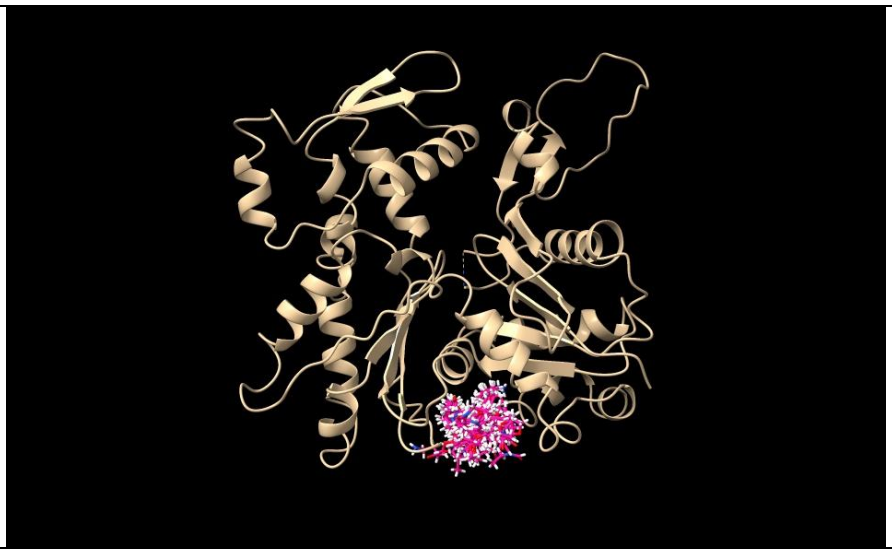

4.2 Binding affinity is not significantly different between different groups

Docking affinities did not differ significantly across receptor conformations (AMPPNP-bound vs ADP-bound actin protomers) or docking box sizes. This is consistent with prior structural studies indicating that actin conformation is governed primarily by polymerization state rather than nucleotide identity. These results suggest that docking scores alone are insufficient to discriminate ligand potency or binding plausibility in this system.

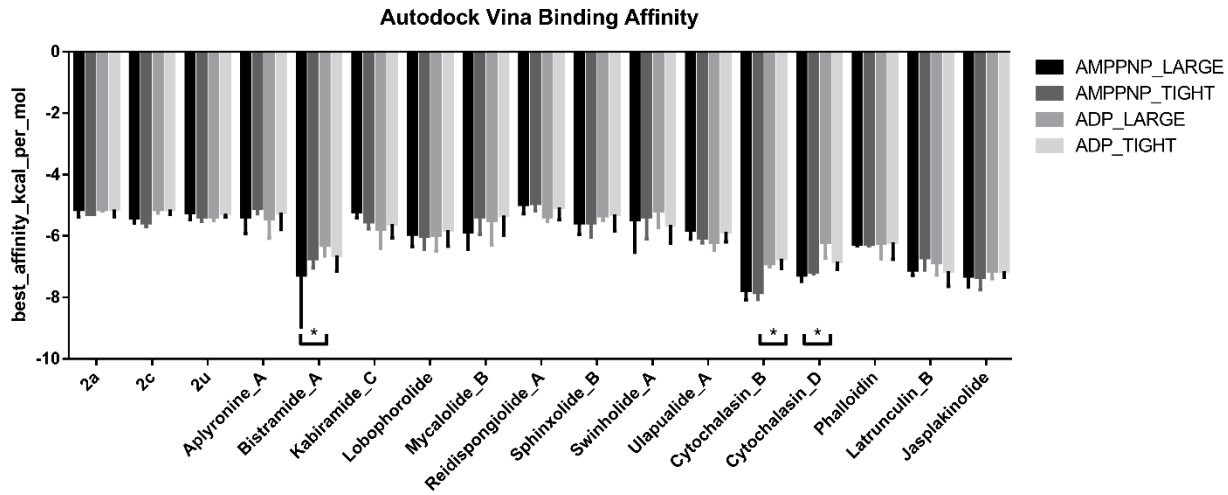

4.3 Potency prediction

To explore whether docking-derived structural features could inform ligand potency, steric clashes between docked ligands and adjacent F-actin protomers (chains A+C) were quantified at distance cutoffs of 0.4, 0.6, and 0.8 Å using ChimeraX. These clash metrics,

together with docking affinity and RDKit-derived ligand descriptors (cLogP, TPSA, molecular weight, hydrogen bond donors/acceptors), were used to train a logistic regression classifier. After excluding three negative control ligands, the model achieved a ROC-AUC of **0.9 ± 0.2**, which is reasonable given the small dataset (n = 14). This analysis suggests that steric compatibility with the polymerization interface may contribute to potency beyond docking score alone.

4.4 RMSD stays high

RMSD between docked poses and crystal ground truth structures remained high (8–12 Å) when evaluated on full ligand heavy atoms, exemplified by ligand 2a. This indicates that Vina docking does not reproduce crystallographic poses for large, flexible macrolides under a rigid-receptor approximation. Likely contributors include (i) receptor state mismatch (F-actin vs G-actin), (ii) limited receptor flexibility in docking, and (iii) challenges associated with macrocyclic ligands.

pose	1	2	3	4	5	6	7
RMSD (Å)	8.508	12.295	12.480	10.543	9.243	9.406	11.830

4.5 Tail contact recovery differs strongly by receptor state

To disentangle pose plausibility from global RMSD, docking was repeated using a G-actin monomer receptor for reidispongiolide A, which has an available crystal structure with consistent atom mapping. Although RMSD remained high across receptor states (~9–12 Å), visual inspection indicated that several docked poses occupied a similar cleft as the crystal ligand, with systematic shifts.

ReidispongiolideA (docking with F-actin, 6DJM) Black: ground truth Orange, yellow, blue: docking poses	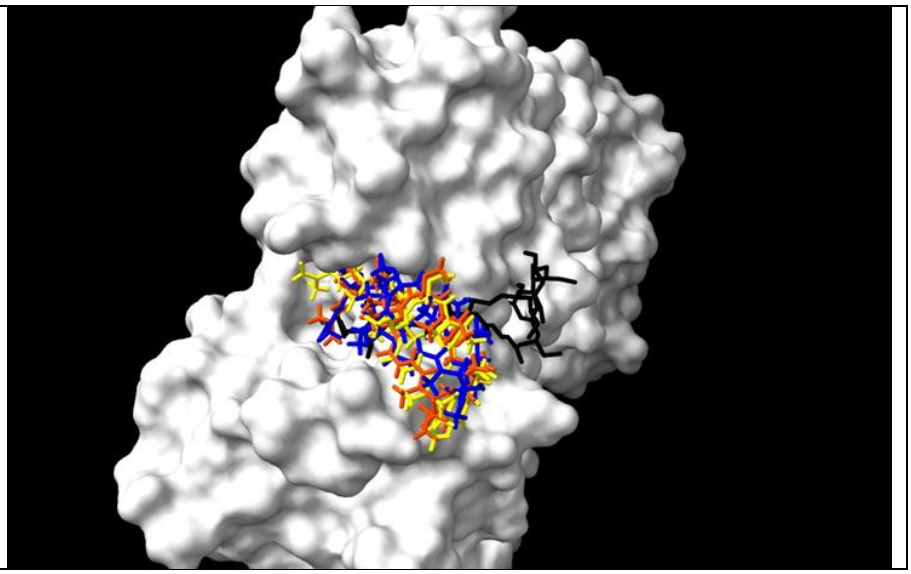

ReidispongiolideA (docking with G-actin, 6MGO) Black: ground truth Orange, yellow, blue: docking poses	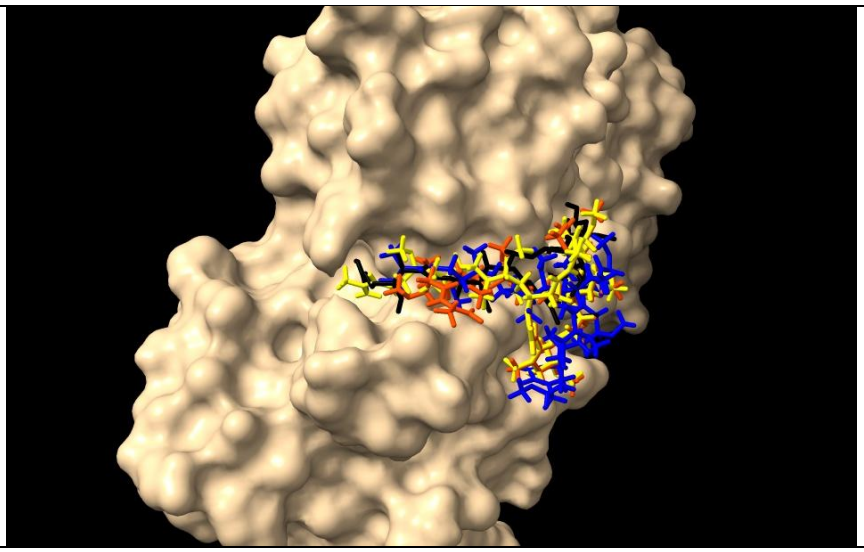

Focusing on the conserved tail region, RMSD and protein–ligand contacts within 4 Å were computed for tail heavy atoms only. In the G-actin receptor, docked poses recovered tail–pocket contact counts comparable to the crystal ground truth (42–46 contacts). In contrast, docking into the AMPPNP/F-actin receptor yielded substantially fewer contacts (33–42 vs 77 in the ground truth). These results demonstrate that receptor conformation strongly influences pose family and interaction plausibility, even when whole-ligand RMSD fails to distinguish outcomes.

	RMSD of G-actin docking	Contact count of G-actin docking	RMSD of F-actin docking	Contact count of F-actin docking
Ground Truth	0	46	0	77
Pose 1	10.225	42	12.347	33
Pose 2	9.414	24	11.909	42
Pose 3	9.244	36	12.556	37

5. Limitations and future directions

5.1 Model limitations

This study uses simplified structural models that do not fully capture the dynamic nature of actin polymerization. In particular, modeling steric clashes between flattened F-actin protomers is an imperfect proxy for barbed-end blocking, which in reality involves incoming G-actin monomers and transient D-loop rearrangements. Additionally, filament severing and intercalation mechanisms (critical determinants of toxin potency) are not addressed by rigid docking and would require molecular dynamics simulations.

Future work could incorporate receptor ensemble docking, explicit solvent modeling, and MD-based relaxation to better capture induced fit and polymerization-state transitions. Alternative docking engines optimized for macrocycles may also improve pose recovery and reduce RMSD.